

Next-to-Leading-Order QCD corrections to $J/\psi(\Upsilon) + \gamma$ production at the LHC

Rong Li and Jian-Xiong Wang

Institute of High Energy Physics, Chinese Academy of Sciences,

P.O. Box 918(4), Beijing, 100049, China.

Theoretical Physics Center for Science Facilities, CAS, Beijing, 100049, China.

(Dated: November 2, 2018)

Abstract

In this work, we calculate the next-to-leading-order (NLO) QCD corrections to the process $p + p \rightarrow J/\psi + \gamma$ via the color-singlet mechanism at the LHC. The results show that the partial cross section ($p_t^{J/\psi} > 3\text{GeV}$ and $|y^{J/\psi,\gamma}| < 3$) is enhanced by a factor of about 2.0, and the differential cross section can be enhanced by two orders of magnitude in the large transverse momentum region of J/ψ . Furthermore, the polarization of J/ψ changes from transverse polarization at leading-order to longitudinal polarization at NLO. For the inclusive J/ψ hadroproduction, it is known that the color-octet contributions are one order of magnitude larger than the color-singlet contribution, and the polarization distribution is dominated by the color-octet behavior at NLO. In contrast, for $J/\psi + \gamma$ production the color-singlet contribution is of the same order as the color-octet contribution, and the polarization distribution arises from both the color-singlet and color-octet. Therefore, measurements of J/ψ production associated with a direct photon at the hadron collider could be an important supplement to testify the theoretical framework treating with the heavy quarkonium. In addition, an NLO QCD correction to $\Upsilon + \gamma$ production at the LHC is also presented in this paper.

PACS numbers: 12.38.Bx, 13.25.Gv, 13.60.Le

For a long time, the productions and decays of heavy quarkonium have been an ideal laboratory to investigate quantum chromodynamics. The large mass of the heavy quarks provides a large scale for production and decay processes. This large scale makes the factorization of the calculations for these processes available, and the hard part in the calculations can be calculated perturbatively. Conventionally, the color-singlet mechanism(CSM) [1] was used to describe the production and decay of heavy quarkonium. However, the CSM has encountered many difficulties in various theoretical[2] and experimental aspects[3]. In 1995, non-relativistic quantum chromodynamics(NRQCD) was put forward[4]. By including the contributions from the high Fock states, NRQCD can overcome the theoretical difficulties[5]. At the same time, the NRQCD predictions are consistent with experimental data[6]. Although NRQCD has had many successes, there are also many problems in the production of heavy quarkonium[7].

In 1995, Kramer calculated the NLO QCD corrections to inclusive J/ψ photoproduction and found that the data from HERA could be understood by just including the high order QCD corrections in CSM [8]. Recently, many studies [9, 10] have shown that NLO QCD corrections in CSM to J/ψ related production processes at B-factory change the theoretical predictions dramatically. Furthermore, at the Tevatron, the NLO QCD corrections in CSM enhance the total cross section by a factor of 2 and give large values for the transverse momentum p_t distribution of J/ψ , especially in the large p_t region[11, 12]. The polarization status of J/ψ drastically changes from transverse-polarization dominant at leading-order (LO) into longitudinal-polarization dominant at NLO for J/ψ hadroproduction[12, 13]. Artoisenet and his collaborators suggested that the p_t distribution of $\Upsilon(1S)$ at the Tevatron can be interpreted in the CSM by taking the NNLO real part into account [14]. It is quite clear that higher order QCD corrections play a very important role in theoretical predictions for the production of heavy quarkonium, and their effects should be carefully investigated in all the relevant processes.

In the framework of CSM, the associated production of $J/\psi + \gamma$ at a hadron collider was first proposed as a good channel to investigate the gluon distribution in the proton with a relatively clean signal[15]. Soon thereafter, it was used to study the polarized gluon distribution[16] and the production mechanism of heavy quarkonium[17]. In reference [18], the associated production of $J/\psi + \gamma$ at the Tevatron has been considered in the CSM at the LO, and the results show that the contribution from gluon fusion process is dominant

over that from the fragmentation processes. Kim investigated the contribution of color-octet processes to the hadroproduction of $J/\psi + \gamma$ and found that the color-octet contributions are dominant in the large p_t region[19]. The contribution from fragmentation processes is smaller than the fusion contribution within the NRQCD framework at the LHC[20]. In reference [21], the authors obtained a theoretical prediction for $J/\psi + \gamma$ hadroproduction at the hadron collider, and the numerical results show that the transverse momentum distribution of J/ψ production is smaller in the CSM than that in the color-octet mechanism (COM) in the large p_t region at LO. To further study the effect of the NLO QCD corrections on heavy quarkonium hadroproduction, in this paper we calculate the NLO QCD corrections to $J/\psi + \gamma$ hadroproduction at the LHC and present theoretical predictions for the p_t distribution of the production and polarization for J/ψ .

We employ the automated Feynman Diagram Calculation package (FDC) to perform the analytic evaluation of all the processes. FDC is a powerful program based on the LISP language designed to automate the NLO calculation and was initially developed by Wang[22]. Its one-loop part was recently completed by Wang and Gong [23]. It has recently been successfully applied to several quarkonium production processes [10, 12, 13, 24, 25].

For the process $p + p \rightarrow J/\psi + \gamma$ at LO, only the gluon fusion process $g + g \rightarrow J/\psi + \gamma$ contributes at the partonic level with six Feynman diagrams, which is similar to that of $g + g \rightarrow J/\psi + g$ in inclusive J/ψ hadroproduction. The LO total cross section is obtained by convoluting the partonic cross section with the parton distribution function (PDF) $G_g(x, \mu_f)$ in the proton:

$$\sigma^B = \int dx_1 dx_2 G_g(x_1, \mu_f) G_g(x_2, \mu_f) \hat{\sigma}^B, \quad (1)$$

where μ_f is the factorization scale. In the following, $\hat{\sigma}$ represents the corresponding partonic cross section.

When the cross section is expanded to NLO on α_s , the coupling constant of quantum chromodynamics, there are one virtual correction and three real correction processes. They are listed as the following:

$$g + g \rightarrow J/\psi + \gamma, \quad (2)$$

$$g + g \rightarrow J/\psi + \gamma + g, \quad (3)$$

$$q(\bar{q}) + g \rightarrow J/\psi + \gamma + q(\bar{q}), \quad (4)$$

$$q + \bar{q} \rightarrow J/\psi + \gamma + g. \quad (5)$$

In calculating the virtual corrections in Eq.(2), there are 111 Feynman diagrams at NLO. The ultraviolet (UV) and infrared (IR) singularities are normalized and separated by using the dimensional regularization. Furthermore, the same renormalization scheme as in Ref. [12, 13] is applied to redefine the quark mass, coupling constant and the quark or gluon fields, and then the renormalized amplitude without UV singularities is obtained. The Coulomb singularity, which comes from the diagrams with a virtual gluon connecting the quark and anti-quark pair in J/ψ , is regulated by introducing a small relative velocity v between the quark and anti-quark pair and is absorbed into the redefinition of the wave function of J/ψ . Therefore, the one-loop amplitude M^V is free of UV and Coulomb singularities and the virtual corrections to the NLO cross section are expressed as

$$\frac{d\hat{\sigma}^V}{dt} \propto 2\text{Re}(M^B M^{V*}), \quad (6)$$

where M^B is the amplitude at LO. It is UV and Coulomb finite, but has IR singularities. To obtain an infrared-safe cross section, it is needed to cancel the IR singularities by adding the contributions from real processes at NLO.

For the real processes in Eqs.(3), (4) and (5), there are IR singularities in the phase space integration which are divided into soft and collinear singularities. The soft singularity is from a soft gluon emitting from the initial gluons. The collinear singularity is from the initial gluon (or quark) emitting a gluon which is nearly parallel to the parent particle. It is easy to find that soft singularities caused by emitting soft gluons from the charm quark-antiquark pair in J/ψ are canceled by each other. Using the standard two cut-off slicing method[26], we decompose the phase space into three regions by introducing two small cutoffs δ_s and δ_c . Therefore, convoluting the parton level cross section with the parton distribution function, the cross section of the real processes is represented as

$$\sigma^R = \sigma^{H\bar{C}} + \sigma^S + \sigma^{HC} + \sigma_{add}^{HC}. \quad (7)$$

Here $\sigma^{H\bar{C}}$ is the contribution from the hard noncollinear part of the phase space that is IR finite, σ^S is the soft part and σ^{HC} is the hard collinear part. After absorbing the mass factorization parts into the PDFs, there is a finite term σ_{add}^{HC} remaining which is similar to that in Eq.(43) in Ref.[13]. By adding all the contributions together, a finite total cross section is obtained.

The polarization of J/ψ is an important physical measurement to identify different production mechanisms. Therefore, the polarization is calculated at NLO. Here we describe the

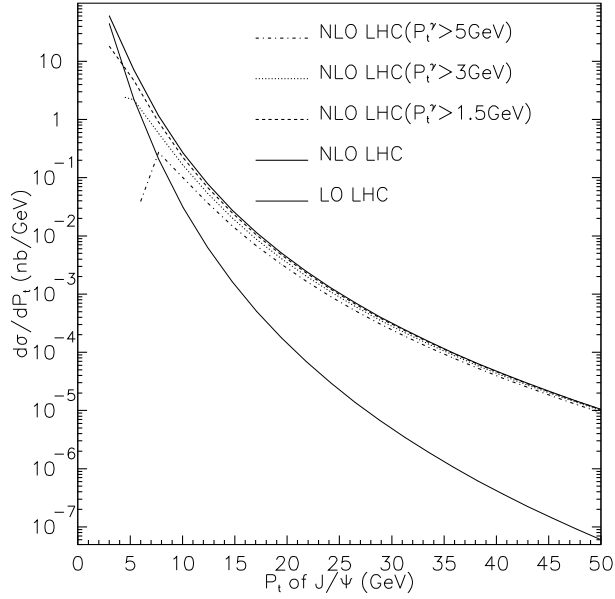


FIG. 1: Transverse momentum distribution of J/ψ production with $\mu_r = \mu_f = \sqrt{(2m_c)^2 + p_t^2}$ at the LHC.

decay of J/ψ in its rest frame with the 3-momentum direction of J/ψ as the z-axis. The polarization parameter α is defined as

$$\alpha(p_t) = \frac{d\sigma_T/dp_t - 2d\sigma_L/dp_t}{d\sigma_T/dp_t + 2d\sigma_L/dp_t}, \quad (8)$$

where σ_T and σ_L are the cross sections of transversely and longitudinally polarized J/ψ respectively. $\alpha = -1$ corresponds to fully longitudinal polarization and $\alpha = 1$ to fully transverse polarization.

To check the gauge invariance for each subprocess, the polarization vectors are replaced by the corresponding momentum in the numerical calculation and the gauge invariance is obviously observed at double precision level. Since the two phase space cutoffs are chosen to handle the IR singularities of the real processes, we varied the cutoffs by a few orders of magnitude to numerically check the independence of the results from the cutoffs and obtained consistent results within the error tolerance.

In the numerical calculation, we use $\alpha=1/137$, $m_c=1.5\text{GeV}$, and $M_{J/\psi} = 2m_c$. From the leptonic width of J/ψ , the wave function at the origin is extracted by

$$\Gamma_{ee} = \left(1 - \frac{16\alpha_s}{3\pi}\right) \frac{16\pi\alpha^2 e_c^2}{M_{J/\psi}^2} |R(0)|^2. \quad (9)$$

We obtain $|R_{J/\psi}(0)|^2=0.944\text{GeV}^3$ at $\alpha_s = \alpha_s(M_{J/\psi}) = 0.26$, $\Gamma_{ee} = 5.55\text{keV}$. The Cteq6L1 and Cteq6M[27] are used in the calculations at LO and NLO respectively, with the corresponding α_s running formula in Cteq6 being used. The renormalization scale μ_r and the factorization scale μ_f are set to $\mu_r = \mu_f = \sqrt{(2m_c)^2 + p_t^2}$. The center-of-mass energy at the LHC is 14TeV and the rapidity cuts for both $J/\psi(\Upsilon)$ and the direct photon are chosen as $|y| < 3$. Because the perturbative expansion does not work well in the small transverse momentum region and the large rapidity region, we impose p_t and y cuts on the numerical calculation. In these processes, the direct photon has nothing to do with the infrared singular structure, so it can be identified with any experimentally acceptable kinematic cuts. Our numerical calculation is obviously consistent with this expectation. Of course, the cut conditions imposed on the direct photon will affect the numerical results. In the following, we fix the rapidity cut of the photon as $|y| < 3$ and vary its p_t cuts to calculate the numerical results.

By replacing the corresponding parameters as

$$\begin{aligned} m_c &\leftrightarrow m_b, & M_{J/\psi} &\leftrightarrow M_\Upsilon, & e_c &\leftrightarrow e_b \\ R_s(0)^{J/\psi} &\leftrightarrow R_s(0)^\Upsilon, & n_f = 3 &\leftrightarrow n_f = 4, \end{aligned} \quad (10)$$

the results of Υ can be obtained. For the bottom quark mass and the wave function of Υ at the origin, $m_b=4.75\text{GeV}$ and $|R_\Upsilon(0)|^2=7.74\text{GeV}^3$ are used. We use the Eq.(9) to calculate the $|R_\Upsilon(0)|^2$ with $\alpha_s(M_\Upsilon) = 0.18$ and $\Gamma_{\Upsilon \rightarrow ee} = 1.34\text{keV}$.

The p_t distribution of J/ψ with different p_t cut conditions on the associated photon is shown in Fig. 1. It is noteworthy that there are two p_t cut conditions, of which one is the J/ψ p_t cut condition and the other is the associated photon p_t cut condition since both J/ψ and the associated photon have to be measured experimentally. The NLO numerical results of the p_t distribution of J/ψ are larger than the LO results by 1 ~ 2 orders of magnitude in the large p_t region, and different cut conditions only affect the results in the region near the minimum endpoint in p_t . In the case of inclusive J/ψ hadroproduction at NLO in COM [24], the results show that the NLO QCD corrections change the results by about 10 percent. Therefore, we can expect that the NLO QCD corrections will modify the results of $J/\psi + \gamma$ at NLO in COM slightly, since the process is quite similar to inclusive J/ψ hadroproduction at NLO in COM. Fig. 2 shows that the NLO QCD corrections also change the p_t distribution of Υ , but with less enhancement than that of J/ψ .

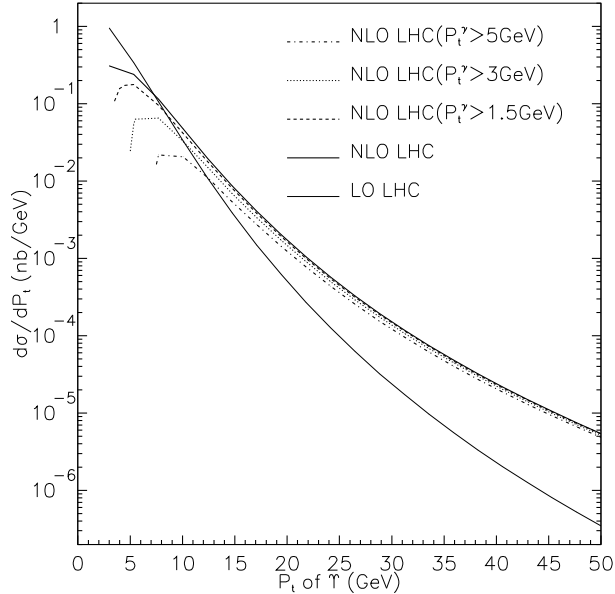


FIG. 2: Transverse momentum distribution of Υ production with $\mu_r = \mu_f = \sqrt{(2m_b)^2 + p_t^2}$ at the LHC.

The theoretical predictions of the J/ψ polarization at NLO are presented in Fig. 3 with different cut conditions. They are similar to the result of J/ψ inclusive hadroproduction. The J/ψ polarization drastically changes from the more transverse polarization at LO to a more longitudinal polarization at NLO. Also, the polarization parameter α of J/ψ at NLO becomes closer to -0.9 as p_t increases. In the figures, the different curves are plotted with different p_t cut conditions. It is clear that the p_t cut condition for the associated photon has a greater effect near the minimum endpoint of J/ψ p_t and a smaller effect in the large p_t region. From Fig. 4, the polarization of Υ also changes from transverse-polarization dominant to longitudinal-polarization dominant, and α at NLO becomes closer to -0.8 as p_t increase. In the small p_t region, the convergence of the numerical calculation becomes worse, and it requires too much CPU time to improve the precision of the calculations. At the same time, the denominator of α changes its sign in the neighborhood of a p_t point in the small p_t region, meaning that the value of α undergoes a vast change around that point. The small value of the denominator also amplifies the error in the calculation, indicating that the convergence of the perturbative expansion is bad and that higher order contributions are important in the small p_t region, especially for the p_t distribution of the polarization parameter α . Therefore, the small p_t region is further discarded in our presentation of α .

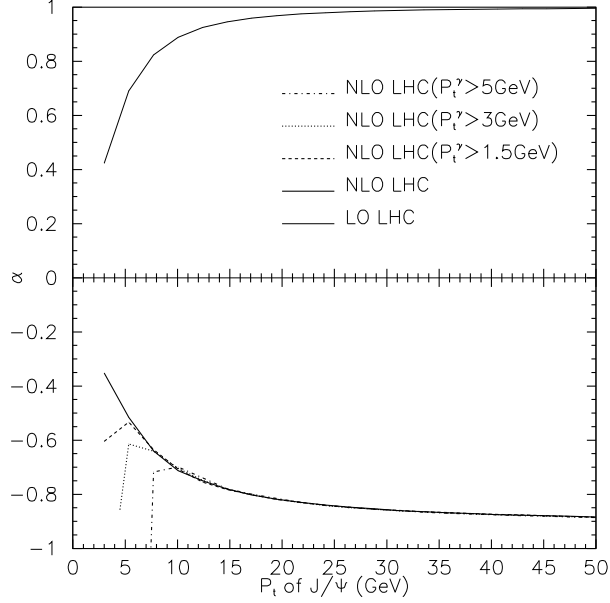


FIG. 3: Transverse momentum dependence of J/ψ polarization with $\mu_r = \mu_f = \sqrt{(2m_c)^2 + p_t^2}$ at the LHC.

In Fig. 5, the μ dependence of the partial cross section ($p_t^{J/\psi(\Upsilon)} > 3\text{GeV}, |y| < 3$) for $J/\psi(\Upsilon) + \gamma + X$ production at LO and NLO are shown with our default choice, $\mu_r = \mu_f = \mu$. In other words, the factorization scale equals to the renormalization scale, and μ ranges from $\mu_0/2$ to $8\mu_0$. There is no p_t cut for the associated photon. It is obvious that QCD corrections reduce the μ dependence of the partial cross section for J/ψ production and moderate the μ dependence for Υ production.

To illustrate the influence of the cut conditions on the partial cross section, we present LO and NLO partial cross sections for $J/\psi(\Upsilon) + \gamma + X$ production at the LHC with different cut conditions in Table I. In Fig. 6, we plot the dependence of the partial cross section on the p_t cut of the direct photon with the p_t cut of $J/\psi(\Upsilon)$ fixed at 10GeV. The plots show that the contributions from small p_t photon are large and the partial cross section decreases as the p_t cut on the photon increases. For the production of Υ , when the p_t cut on the photon becomes too close to the p_t cut of Υ , the partial cross section decreases rapidly and the influence of the error becomes severe. In this case, too many contributions from the real processes are cut off and the perturbative calculation becomes worse. Therefore, the partial cross section cannot be taken seriously when the p_t cut condition of the photon approaches the p_t cut condition of Υ .

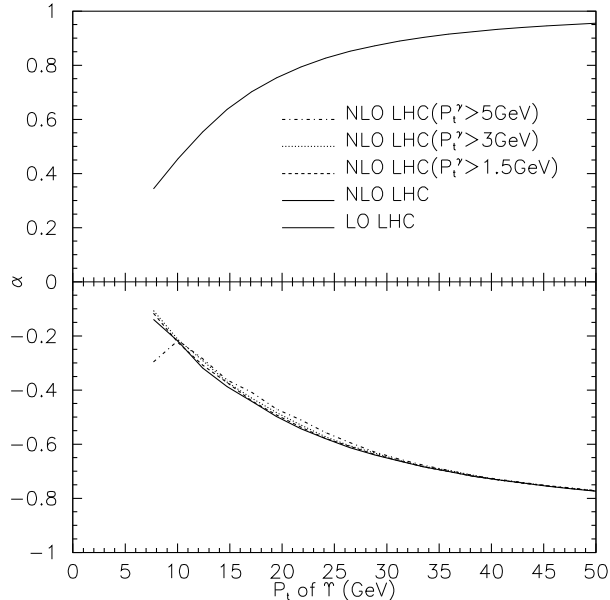


FIG. 4: Transverse momentum dependence of Υ polarization with $\mu_r = \mu_f = \sqrt{(2m_b)^2 + p_t^2}$ at the LHC.

In summary, we have calculated NLO QCD corrections to the production of $J/\psi(\Upsilon)$ associated with a direct photon at the LHC in CSM. For J/ψ production, the partial cross section is enhanced by a factor of about 2.0 with J/ψ transverse momentum cut $p_t > 3\text{GeV}$ and rapidity cut $|y| < 3$ for both J/ψ and the direct photon. The transverse momentum distribution of J/ψ at NLO is enhanced by 1 \sim 2 orders of magnitude over LO calculations as p_t becomes larger. The J/ψ polarization is calculated, and the results show that the J/ψ polarization drastically changes from transverse-polarization dominant at LO to longitudinal-polarization dominant at NLO. The situation is quite similar to the case of NLO QCD corrections to the inclusive J/ψ hadroproduction. It can be seen that NLO results on $J/\psi + \gamma$ hadroproduction in CSM is of the same order of magnitude as LO results in COM[19, 21]. As a reasonable estimate from the experience of NLO QCD correction calculation to inclusive J/ψ hadroproduction in COM[24], the NLO p_t distribution for $J/\psi + \gamma$ hadroproduction in COM will be changed slightly and the polarization will remain almost the same. Therefore, the results of J/ψ production associated with a direct photon from the CSM and COM are of the same order of magnitude at NLO. Therefore, the J/ψ polarization measurement would be able to distinguish the contributions from the CSM and COM since the theoretical predictions of J/ψ polarization are obviously different for the CSM and

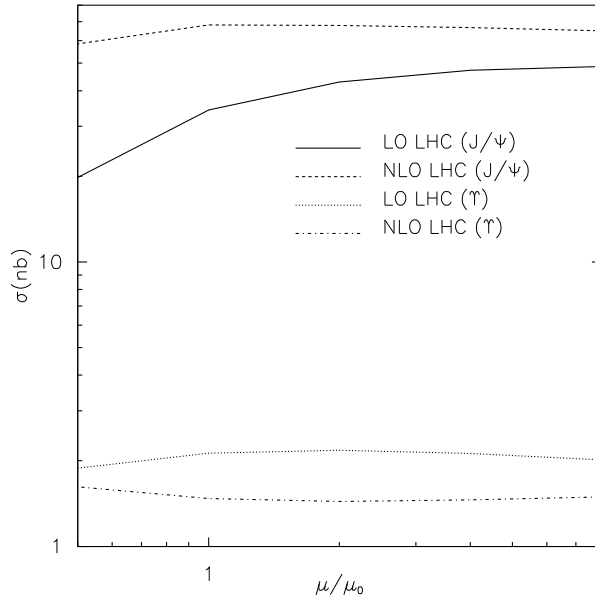


FIG. 5: The μ dependence of the partial cross section ($p_t^{J/\psi(\Upsilon)} > 3\text{GeV}$) with $\mu_0 = \sqrt{(M_{J/\psi(\Upsilon)})^2 + p_t^2}$.

COM. In contrast to the case of J/ψ inclusive hadroproduction, the NLO result of CSM is about one order of magnitude smaller than the NLO result of COM, and so there is no way for the CSM part to play an important role in the final J/ψ polarization distribution.

To measure the production of $J/\psi(\Upsilon)$ associated with a direct photon at the LHC, the direct photon must be identified. To cut the enormous background of photons emitted in jet hadronization, photons from jets are attributed to the jets and a direct photon, which is isolated from any jets, should be identified. Therefore, being quite different from $J/\psi(\Upsilon)$ inclusive hadroproduction, the hadroproduction of $J/\psi(\Upsilon)$ associated with a direct photon will be an important process to investigate the production mechanism of heavy quarkonium and impose new constraints on the contribution of COM to heavy quarkonium hadroproduction.

We thank Gong Bin for helpful discussions. This work is supported by the National Natural Science Foundation of China (No. 10775141) and by the Chinese Academy of Sciences

TABLE I: The partial cross section at LO and NLO with different cut conditions for transverse momentum p_t but fixed rapidity cut condition $|y| < 3$ for both $J/\psi(\Upsilon)$ and the direct photon. (units: $p_t(\text{GeV})$, $\sigma(\text{nb})$)

p_t^γ	$p_t^{J/\psi}$	$\sigma_{LO}^{J/\psi}$	$\sigma_{NLO}^{J/\psi}$	$K_{J/\psi}$	p_t^Υ	σ_{LO}^Υ	σ_{NLO}^Υ	K_Υ
> 0.0	> 3.0	34	68	2.0	> 3.0	2.1	1.5	0.71
> 1.5	> 3.0	34	34	1.0	> 3.5	1.7	0.94	0.55
> 3.0	> 4.5	5.5	6.0	1.1	> 5.0	0.82	0.46	0.56
> 5.0	> 6.0	1.2	1.2	1.0	> 7.5	0.24	0.16	0.67

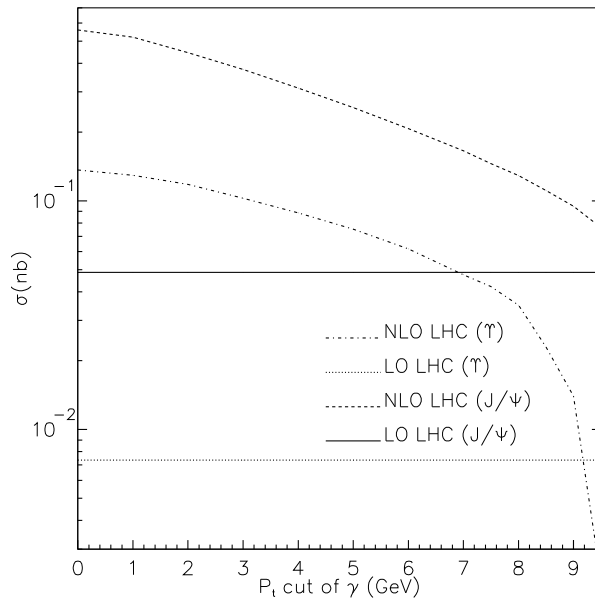


FIG. 6: The partial cross section of the $J/\psi(\Upsilon)$ production associated with a direct photon as a function of p_t cuts of the photon at the LHC. Here we fix the low bound of the $J/\psi(\Upsilon)$'s p_t at 10GeV

under Project No. KJCX3-SYW-N2.

- [1] M. B. Einhorn and S. D. Ellis, Phys. Rev. **D12**, 2007 (1975); S. D. Ellis, M. B. Einhorn, and C. Quigg, Phys. Rev. Lett. **36**, 1263 (1976); C.-H. Chang, Nucl. Phys. **B172**, 425 (1980); E. L. Berger and D. L. Jones, Phys. Rev. **D23**, 1521 (1981); R. Baier and R. Ruckl, Nucl. Phys. **B201**, 1 (1982).
- [2] R. Barbieri, R. Gatto, and E. Remiddi, Phys. Lett. **B61**, 465 (1976); R. Barbieri, M. Caffo, R. Gatto, and E. Remiddi, Phys. Lett. **B95**, 93 (1980); R. Barbieri, M. Caffo, R. Gatto, and E. Remiddi, Nucl. Phys. **B192**, 61 (1981); R. Barbieri, E. d’Emilio, G. Curci, and E. Remiddi, Nucl. Phys. **B154**, 535 (1979); K. Hagiwara, C. B. Kim, and T. Yoshino, Nucl. Phys. **B177**, 461 (1981); P. B. Mackenzie and G. P. Lepage, Phys. Rev. Lett. **47**, 1244 (1981).
- [3] F. Abe et al. (CDF), Phys. Rev. Lett. **69**, 3704 (1992); F. Abe et al. (CDF), Phys. Rev. Lett. **71**, 2537 (1993).
- [4] G. T. Bodwin, E. Braaten, and G. P. Lepage, Phys. Rev. **D51**, 1125 (1995), hep-ph/9407339.
- [5] G. T. Bodwin, E. Braaten, and G. P. Lepage, Phys. Rev. **D46**, 1914 (1992), hep-lat/9205006.
- [6] E. Braaten and T. C. Yuan, Phys. Rev. **D50**, 3176 (1994), hep-ph/9403401; E. Braaten and S. Fleming, Phys. Rev. Lett. **74**, 3327 (1995), hep-ph/9411365; P. L. Cho and A. K. Leibovich, Phys. Rev. **D53**, 150 (1996), hep-ph/9505329; P. L. Cho and A. K. Leibovich, Phys. Rev. **D53**, 6203 (1996), hep-ph/9511315.
- [7] N. Brambilla et al. (Quarkonium Working Group) (2004), hep-ph/0412158; J. P. Lansberg, Int. J. Mod. Phys. **A21**, 3857 (2006), hep-ph/0602091; X.-Q. Li, X. Liu, and Z.-T. Wei (2008), 0808.2587.
- [8] M. Kramer, Nucl. Phys. **B459**, 3 (1996), hep-ph/9508409; M. Kramer, Prog. Part. Nucl. Phys. **47**, 141 (2001), hep-ph/0106120.
- [9] Y.-J. Zhang, Y.-j. Gao, and K.-T. Chao, Phys. Rev. Lett. **96**, 092001 (2006), hep-ph/0506076; Y.-J. Zhang and K.-T. Chao, Phys. Rev. Lett. **98**, 092003 (2007), hep-ph/0611086; Y.-J. Zhang, Y.-Q. Ma, and K.-T. Chao, Phys. Rev. **D78**, 054006 (2008), 0802.3655.
- [10] B. Gong and J.-X. Wang, Phys. Rev. **D77**, 054028 (2008), 0712.4220; B. Gong and J.-X. Wang, Phys. Rev. Lett. **100**, 181803 (2008), 0801.0648.
- [11] J. Campbell, F. Maltoni, and F. Tramontano, Phys. Rev. Lett. **98**, 252002 (2007), hep-

ph/0703113.

- [12] B. Gong and J.-X. Wang, Phys. Rev. Lett. **100**, 232001 (2008), 0802.3727.
- [13] B. Gong and J.-X. Wang, Phys. Rev. **D78**, 074011 (2008), 0805.2469.
- [14] P. Artoisenet, J. Campbell, J. P. Lansberg, F. Maltoni, and F. Tramontano, Phys. Rev. Lett. **101**, 152001 (2008), 0806.3282.
- [15] M. Drees and C. S. Kim, Z. Phys. **C53**, 673 (1992).
- [16] M. A. Doncheski and C. S. Kim, Phys. Rev. **D49**, 4463 (1994), hep-ph/9303248.
- [17] C. S. Kim and E. Mirkes, Phys. Rev. **D51**, 3340 (1995), hep-ph/9407318; E. Mirkes and C. S. Kim, Phys. Lett. **B346**, 124 (1995), hep-ph/9504412.
- [18] D. P. Roy and K. Sridhar, Phys. Lett. **B341**, 413 (1995), hep-ph/9407390.
- [19] C. S. Kim, J. Lee, and H. S. Song, Phys. Rev. **D55**, 5429 (1997), hep-ph/9610294.
- [20] P. Mathews, K. Sridhar, and R. Basu, Phys. Rev. **D60**, 014009 (1999), hep-ph/9901276.
- [21] B. A. Kniehl, C. P. Palisoc, and L. Zvirner, Phys. Rev. **D66**, 114002 (2002), hep-ph/0208104.
- [22] J.-X. Wang, Nucl. Instrum. Meth. **A534**, 241 (2004), hep-ph/0407058.
- [23] B. Gong and J.-X. Wang (2008), in preparation.
- [24] B. Gong, X. Q. Li, and J.-X. Wang (2008), 0805.4751.
- [25] B. Gong, Y. Jia, and J.-X. Wang (2008), 0808.1034.
- [26] B. W. Harris and J. F. Owens, Phys. Rev. **D65**, 094032 (2002), hep-ph/0102128.
- [27] J. Pumplin et al., JHEP **07**, 012 (2002), hep-ph/0201195.